Published in "Inorganic Chemistry 45(2): 660 -668, 2006"
which should be cited to refer to this work.

(Strept)avidin as Host for Biotinylated Coordination Complexes: Stability, Chiral Discrimination, and Cooperativity

Andreas Loosli,[†] Untung Edy Rusbandi,[†] Julieta Gradinaru,[†] Klaus Bernauer,[†] Carl Wilhelm Schlaepfer,[‡] Michel Meyer,[§] Sylwester Mazurek,[†,||] Marjana Novic,[||] and Thomas R. Ward*,[†]

Institute of Chemistry, University of Neuchâtel, Av. Bellevaux 51, CP 2, CH-2007 Neuchâtel, Switzerland, Institute of Inorganic Chemistry, University of Fribourg, Pérolles, CH-1700 Fribourg, Switzerland, Laboratoire d'Ingénierie Moléculaire pour la Séparation et les Applications des Gaz (LIMSAG, UMR 5633 du CNRS), Université de Bourgogne, Faculté des Sciences, 6 Boulevard Gabriel, F-21100 Dijon, France, and Laboratory of Chemometrics, National Institute of Chemistry, Hajdrihova 19, SI-1001 Ljubljana, Slovenia

Incorporation of a biotinylated ruthenium tris(bipyridine) $[Ru(bpy)_2(Biot\text{-}bpy)]^{2+}$ (**1**) in either avidin or streptavidin—(strept)avidin—can be conveniently followed by circular dichroism spectroscopy. To determine the stepwise association constants, cooperativity, and chiral discrimination properties, diastereopure (Λ and Δ)-**1** species were synthesized and incorporated in tetrameric (strept)avidin to afford $(\Delta\text{-}[Ru(bpy)_2(Biot\text{-}bpy)]^{2+})_x\subset$avidin, $(\Lambda\text{-}[Ru(bpy)_2(Biot\text{-}bpy)]^{2+})_x\subset$avidin, $(\Delta\text{-}[Ru(bpy)_2(Biot\text{-}bpy)]^{2+})_x\subset$streptavidin, and $(\Lambda\text{-}[Ru(bpy)_2(Biot\text{-}bpy)]^{2+})_x\subset$streptavidin ($x = 1$–4) For these four systems, the overall stability constants are log $\beta_4 = 28.6$, 30.3, 36.2, and 36.4, respectively. Critical analysis of the CD titrations data suggests a strong cooperativity between the first and the second binding event ($x = 1$, 2) and a pronounced difference in affinity between avidin and streptavidin for the dicationic guest **1** as well as modest enantiodiscrimination properties with avidin as host.

Introduction

Over the past 4 decades, the biotin−avidin system has found numerous applications both in research and in technology.[1] The versatility of the biotin−avidin system relies on the extraordinary affinity of biotin for either avidin ($K_a \approx 10^{15}$ M^{-1}) or streptavidin ($K_a \approx 10^{13}$ M^{-1}). [Hereafter, (strept)avidin refers to either avidin or streptavidin.] This places the biotin−(strept)avidin interaction among the strongest noncovalent interactions known in Nature.[2]

Detailed structural and biophysical analyses of the biotin−(strept)avidin system reveal that the extraordinary affinity relies on multiple hydrogen-bonding interactions, coupled with a deep hydrophobic pocket provided by aromatic residues.[3−5] A total of six H-bonds have been identified between the biotin's bicyclic framework and (strept)avidin: five contacts with the urea functionality and one with the thioether. The valeric acid side chain interacts via five H-bonds with avidin but only via two with streptavidin. Three tryptophane and two phenylalanine residues shape a deep hydrophobic pocket in avidin. In streptavidin, a total of four tryptophanes make up the biotin-binding site. In both systems, one critical tryptophane is supplied by an adjacent monomer and shields the binding site. Indeed, (strept)avidin is a homotetrameric β-barrel protein with four equivalent binding sites. In terms of binding events, the question of cooperativity between biotin and tetrameric (strept)avidin is an open debate, some experiments pointing toward cooperative binding, while others seem to favor noncooperative binding.[6−8] Although well preorganized to bind to biotin

* To whom correspondence should be addressed. E-mail: thomas.ward@unine.ch.
[†] University of Neuchâtel.
[‡] University of Fribourg.
[§] Université de Bourgogne.
[||] National Institute of Chemistry.

(1) Wilchek, M., Bayer, E. A., Eds. *Methods in Enzymology: Avidin-Biotin Technology*; Academic Press: San Diego, CA, 1990; Vol. 184.
(2) Rao, J.; Lahiri, J.; Isaacs, L.; Weis, R. M.; Whitesides, G. M. *Science* **1998**, *280*, 708−711.
(3) Livnah, O.; Bayer, E. A.; Wilchek, M.; Sussman, J. L. *Proc. Natl. Acad. Sci. U.S.A.* **1993**, *90*, 5076−5080.
(4) Klumb, L. A.; Chu, V.; Stayton, P. S. *Biochemistry* **1998**, *37*, 7657−7663.
(5) Weber, P. C.; Ohlendorf, D. H.; Wendoloski, J. J.; Salemme, F. R. *Science* **1989**, *243*, 85−88.

(according to the lock-and-key principle), (strept)avidin undergoes subtle structural changes upon biotin binding. In particular, the loop L-3,4 (between β-sheet 3 and β-sheet 4) becomes ordered upon binding thus locking biotin in the binding site. This critical loop contains nine residues (36−44) in avidin but only six residues (45−50) in streptavidin.[3] In avidin, it contributes to three hydrogen bonding contacts with one of the valeric acid side chain. In streptavidin, this loop interacts only via a single hydrogen bond to the valeric acid side chain. Using H−D exchange experiments, coupled to mass spectral analysis, it has been shown that (strept)-avidin undergoes significant tightening upon biotin binding.[9]

In terms of applications, it is generally accepted that derivatization of the valeric acid functionality does not impart too significantly on the affinity of the biotin−(strept)avidin system. In addition, biotinylated probes most often retain their biological and physicochemical properties. These remarkable features allow one to biotinylate nearly any (macro)molecule and then noncovalently incorporate it into (strept)avidin while preserving its properties. As (strept)-avidin consists of four identical eight-stranded β-barrels, different biotinylated molecules can, in principle, be anchored on a single tetramer.[1]

The most common applications of the biotin−avidin technology include diagnostics, immunoassays, affinity targeting, cross-linking agents, immobilizing agents, signal amplification, etc.[1] For all of these applications it is recommended to introduce a long spacer between the biotin anchor and the probe. This guarantees that the probe does not interact significantly with (strept)avidin and, thus, retains most of its properties of interest.

In recent years, however, (strept)avidin has received increasing attention as a host protein for coordination complexes.[10−21] For this purpose, a short spacer is selected, thus ensuring incorporation of the metal within the protein environment. On one hand, various biotinylated coordination complexes with interesting photophysical properties have been incorporated in (strept)avidin. These studies revealed the influence of the protein environment on the excited-state lifetimes of the supramolecular systems.[10−20] On the other hand, biotinylated organometallic catalyst precursors have been tested in enantioselective catalysis. As the first coordination sphere of these catalysts is achiral, the enantiomeric excess of the product resulting from the catalytic transformation can be attributed exclusively to second coordination sphere interactions.[10,16−18] Such systems thus offer a straightforward readout of the influence of second coordination sphere interactions on either photophysical or catalytic properties of the supramolecular architectures.

Shortening the length of the spacer between the biotin anchor and the metal complex to ensure significant contacts between both partners raises the fundamental question of stability of the host−guest supermolecule. Indeed, one can expect that the tetrameric protein must undergo a significant structural reorganization to embrace a large metal complex within its biotin binding site. To address this issue, we have synthesized a biotinylated ruthenium tris(bipyridine) complex and determined its affinity for (strept)avidin. Upon incorporation in the host protein, the complex displays an induced CD signal, which can be exploited to determine whether binding occurs cooperatively and whether there is any chiral discrimination between the host and the guest.

Results and Discussion

Synthesis. As biotinylated probe, we selected the ruthenium tris(bipyridine) complex $[Ru(bpy)_2(Biot\text{-}bpy)]^{2+}$ (**1**). We reasoned that the aromatic first coordination sphere of the probe **1** should find, upon incorporation in (strept)avidin, stabilizing interactions with the aromatic residues lining the protein's binding pocket. In addition, the dicationic charge of the coordination complex may result in pronounced differences in affinity for avidin (pI = 10.4) compared to streptavidin (pI = 6.4), where pI stands for the isoelectric point.

The synthesis of the biotinylated bipyridine ligand Biot-bpy (**4**) was achieved by mixing equimolar amounts of biotinylated ethylenediamine (**2**)[22] with the activated ester (**3**)[23] in the presence of triethylamine in DMF. Refluxing $[Ru(bpy)_2Cl_2]$ in the presence of a slight excess of Biot-bpy (**4**) affords *rac*-$[Ru(bpy)_2(Biot\text{-}bpy)](PF_6)_2$ (*rac*-**1**$(PF_6)_2$), after precipitation with NH_4PF_6 (Scheme 1). All experimental details can be found in the Supporting Information.

The preparation of diastereopure Δ-$[Ru(bpy)_2(Biot\text{-}bpy)]^{2+}$ (Δ-**1**) was achieved using von Zelewsky's procedure.[24] Treatment of Δ-$[Ru(bpy)_2(py)_2][(+)\text{-}O,O'\text{-dibenzoyl-D-tartrate}]$ with Biot-bpy (**4**) in ethyleneglycol-water in the dark affords Δ-$[Ru(bpy)_2(Biot\text{-}bpy)]^{2+}$ (Δ-**1**). The diastereomeric purity of the biotinylated complex Δ-**1** was assessed by subjecting a small crude sample to ion exchange chroma-

(6) Jones, M. L.; Kurzban, G. P. *Biochemistry* **1995**, *34*, 11750−11756.
(7) Sano, T.; Cantor, C. R. *J. Biol. Chem.* **1990**, *265*, 3369−3373.
(8) Gonzales, M.; Bagatolli, L. A.; Echabe, I.; Arrondo, J. L. R.; Argarana, C. E.; Cantor, C. R.; Fidelio, G. D. *J. Biol. Chem.* **1997**, *272*, 11288−11294.
(9) Williams, D. H.; Stephens, E.; Zhou, M. *Chem. Commun.* **2003**, 1973−1976.
(10) Wilson, M. E.; Whitesides, G. M. *J. Am. Chem. Soc.* **1978**, *100*, 306−307.
(11) Lo, K. K.-W.; Chan, J. S.-W.; Lui, L.-H.; Chung, C.-K. *Organometallics* **2004**, *23*, 3108−3116.
(12) Lo, K. K.-W.; Chung, C.-K.; Zhu, N. *Chem. Eur. J.* **2003**, *9*, 475−483.
(13) Lo, K. K.-W.; Lee, T. K.-M. *Inorg. Chem.* **2004**, *43*, 5275−5282.
(14) Lo, K. K.-W.; Hui, W.-K. *Inorg. Chem.* **2005**, *44*, 1992−2002.
(15) Lo, K. K.-W.; Hui, W.-K.; Ng, D. C.-M. *J. Am. Chem. Soc.* **2002**, *124*, 9344−9345.
(16) Collot, J.; Gradinaru, J.; Humbert, N.; Skander, M.; Zocchi, A.; Ward, T. R. *J. Am. Chem. Soc.* **2003**, *125*, 9030−9031.
(17) Skander, M.; Humbert, N.; Collot, J.; Gradinaru, J.; Klein, G.; Loosli, A.; Sauser, J.; Zocchi, A.; Gilardoni, F.; Ward, T. R. *J. Am. Chem. Soc.* **2004**, *126*, 14411−14418.
(18) Letondor, C.; Humbert, N.; Ward, T. R. *Proc. Natl. Acad. Sci. U.S.A.* **2005**, *102*, 4683−4687.
(19) Taki, M.; Murakami, H.; Sisido, M. *Chem. Commun.* **2000**, 1199−1200.
(20) Slim, M.; Sleiman, H. F. *Bioconjugate Chem.* **2004**, *15*, 949−953.
(21) Jhaveri, S. D.; Trammell, S. A.; Lowy, D. A.; Tender, L. M. *J. Am. Chem. Soc.* **2005**, *126*, 6540−6541.
(22) Li, Z.; Ortega-Vilain, A.-C.; Patil, G. S.; Chu, D.-L.; Foreman, J. E.; Eveleth, D. D.; Powers, J. C. *J. Med. Chem.* **1996**, *39*, 4089−4098.
(23) Grammenudi, S.; Franke, M.; Vögtle, F.; Steckhan, E. *J. Inclusion Phenom.* **1987**, *5*, 695−707.
(24) Hua, X.; von Zelewsky, A. *Inorg. Chem.* **1995**, *34*, 5791−5797.

Scheme 1. Biotinylated Ligand Synthesis of Biot-bpy (**4**) and Formation of the Corresponding Racemic Coordination Complex *rac*-$[Ru(bpy)_2(Biot\text{-}bpy)](PF_6)_2$ (*rac*-**1**$(PF_6)_2$)

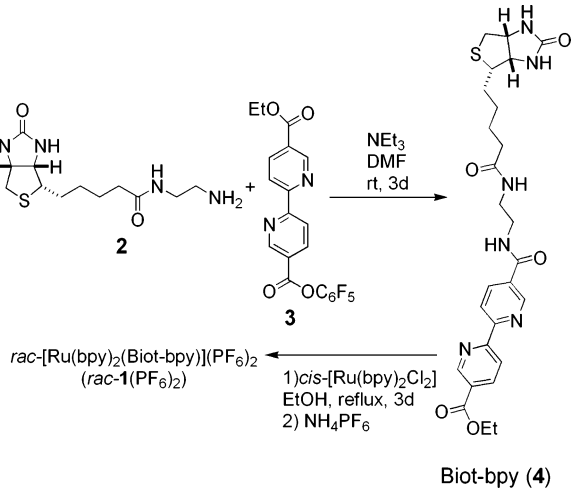

tography (SP Sephadex C-25) using potassium nitrate as eluent (0.05 M, pH = 5.0). The entire elution peak was collected in five fractions, and each of these was analyzed by UV−vis and CD spectroscopy. Plotting the ratio of the signals (UV−vis/CD) for each fraction resulted in a horizontal line, thus suggesting that the entire elution peak is diastereopure.

The epimeric Λ-$[Ru(bpy)_2(Biot\text{-}bpy)]^{2+}$ (Λ-**1**) was obtained similarly from Λ-$[Ru(bpy)_2(py)_2]$[(−)-*O*,*O*′-dibenzoyl-L-tartrate]. The synthesis and CD spectra of Λ-**1** and Δ-**1** are presented in Scheme 2.

Docking Studies. To gain a qualitative insight on the ability of the (strept)avidin to accommodate up to four biotinylated $[Ru(bpy)_2(Biot\text{-}bpy)]^{2+}$ (**1**) probes, docking studies were carried out using the AutoDock algorithm (the implemented Lamarckian genetic algorithm).[25,26] All dockings presented below are based on a rigid host model and thus should be considered as qualitative.

Since tetrameric (strept)avidin consists of a dimer of dimers with two proximal and two distal binding sites, docking studies were carried out on the dimeric structure (with two proximal binding sites) downloaded from the protein data bank (http://www.rcsb.org/pdb/): firstp for streptavidin and 1avd for avidin. The biotinylated complex **1** was built using Hyperchem 7.5 on the basis of the structurally characterized $[Ru(5,5'\text{-}CO_2Et\text{-}2,2'\text{-}bpy)_3](PF_6)_2$[27] as well as the (+)-biotin anchor extracted from (strept)avidin. For docking purposes, the (*Z*)-configuration of both amides in complex **1** was enforced and the geometry of the $[Ru(bpy)_3]^{2+}$ unit was frozen. The dihedral angle of both amide carbonyls was set to $\tau = 0$ and 180° consecutively (Scheme 2, in blue), thus yielding a total of four different ligand conformers, associated with the two epimers at ruthenium (Λ or Δ) to afford a total of eight guests, which were docked in both avidin and streptavidin.[28,29] The optimization procedure was performed by allowing rotation around the four bonds highlighted in red in Scheme 2.

During the first simulation, one diastereopure $[Ru(bpy)_2(Biot\text{-}bpy)]^{2+}$ (**1**) (four possible ligand conformers, blue in Scheme 2) was docked in the (strept)avidin dimer to yield $[Ru(bpy)_2(Biot\text{-}bpy)]^{2+}\subset$(strept)avidin. For each of the eight possible docked guests, the most stable structures (most negative binding enthalpy) were selected and the root-mean-square values (rms) were determined for the biotin bicyclic scaffold and compared to the reported X-ray structure $(biotin)_4\subset$(strept)avidin firstp and 1avd, respectively.

From these qualitative results, there appears to be no significant difference in binding enthalpy between either diastereomer (Λ or Δ)-**1** and (strept)avidin (average binding enthalpy −8.8 kcal·mol^{-1}, average rms 1.1). Inspection of the most stable docked structure $[Ru(bpy)_2(Biot\text{-}bpy)]^{2+}\subset$(strept)avidin reveals the following:

(i) The biotinylated $[Ru(bpy)_3]^{2+}$ moiety shields the second biotin binding site both with avidin and with streptavidin dimers. It should be emphasized that, in the simulation, this second biotin binding site is occupied only during the third binding event in the tetrameric (strept)avidin. Indeed, the second binding event occurs at the distal binding site (see Scheme 3), which is not considered in the docking study.

(ii) In the presence of an ethylenediamine spacer between the anchor and the coordination compound, the $[Ru(bpy)_3]^{2+}$ unit is located on the surface rather than in the binding pocket of (strept)avidin, and this is despite the depth of the binding site.

For the second docking simulation—which corresponds to the third or fourth binding events (K_3 or K_4) as the second binding event occurs at the distal binding site, not considered in this model—a second equivalent of homochiral (Λ or Δ)-**1** was docked to afford $([Ru(bpy)_2(Biot\text{-}bpy)]^{2+})_2\subset$(strept)-avidin (Figure 1). For this second docking procedure, not all of the four possible ligand conformations yielded a minimized structure. The following features emerge:

(ii) This loss of binding energy is associated with significantly larger rms values for biotin's bicyclic framework: 2.7 for the second binding event. This suggests that the host protein must undergo significant reorganization to accommodate the third (and the fourth) biotinylated probes.

In light of the crude model used for the docking simulations, care should be applied when discussing quantitative aspects of the $([Ru(bpy)_2(Biot\text{-}bpy)]^{2+})_x\subset$(strept)avidin interactions. The qualitative three-dimensional model suggests that the ruthenium complex is located on the surface of (strept)avidin rather than in the binding pocket. However, the tetrameric nature of the protein provides a large contact area between the host and the guest.

Titrations. The activity of the host protein was determined using Gruber's protocol on the basis of the fluorescence

(25) Morris, G. M.; Goodsell, D. S.; Halliday, R. S.; Huey, R.; Hart, W. E.; Belew, R. K.; Olson, A. J. *J. Comput. Chem.* **1998**, *19*, 1639−1662.
(26) Goodsell, D. S.; Morris, G. M.; Olson, A. J. *J. Mol. Recognit.* **1996**, *9*, 1−5.
(27) Loosli, A.; Ward, T. R.; Stoeckli-Evans, H. Unpublished result.
(28) Cornell, W. D.; Cieplak, P.; Bayly, C. I.; Gould, I. R.; Merz Jr, K. M.; Ferguson, D. M.; Spellmeyer, D. C.; Fox, T.; Caldwell, J. W.; Kollman, P. A. *J. Am. Chem. Soc.* **1995**, *117*, 5179−5197.
(29) The grid size used for all dockings was set to 80 × 80 × 80 points with a 0.375 Å grid space. The AMBER force-field parameters were used for all atoms, replacing Ru(II) by Zn(II) parameters.

Scheme 2. Synthesis of Diastereopure Biotinylated Coordination Complex Λ-[Ru(bpy)$_2$(Biot-bpy)]$^{2+}$ (Δ-**1**) Using Von Zelewsky's Procedure[a]

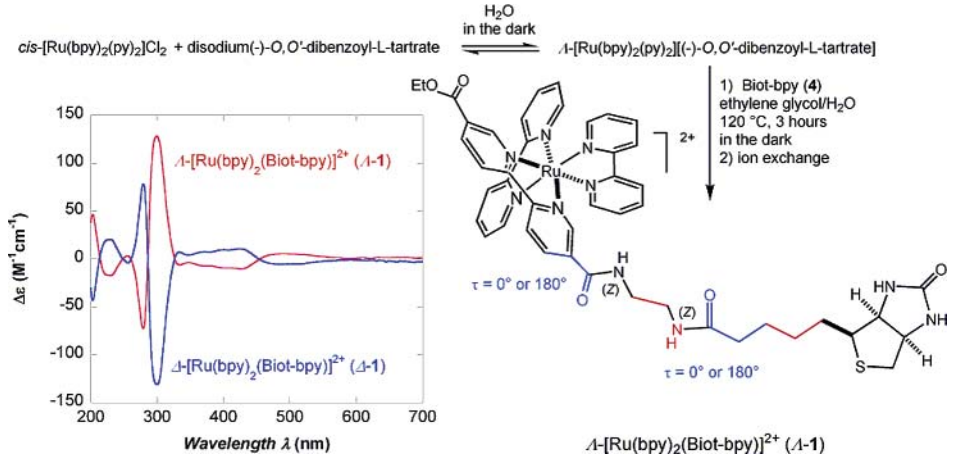

[a] The inset depicts the CD spectra of Λ-**1** (red line) and Δ-**1** (blue line). The rotation around the four bonds highlighted in red was allowed during the docking simulation. The blue dihedral angles were fixed either to $\tau = 0$ or 180°, yielding four possible ligand conformations used for docking.

Scheme 3. Enumeration of All Binding Events for a Racemic Guest *rac*-**1** in a Tetrameric Host Protein[a]

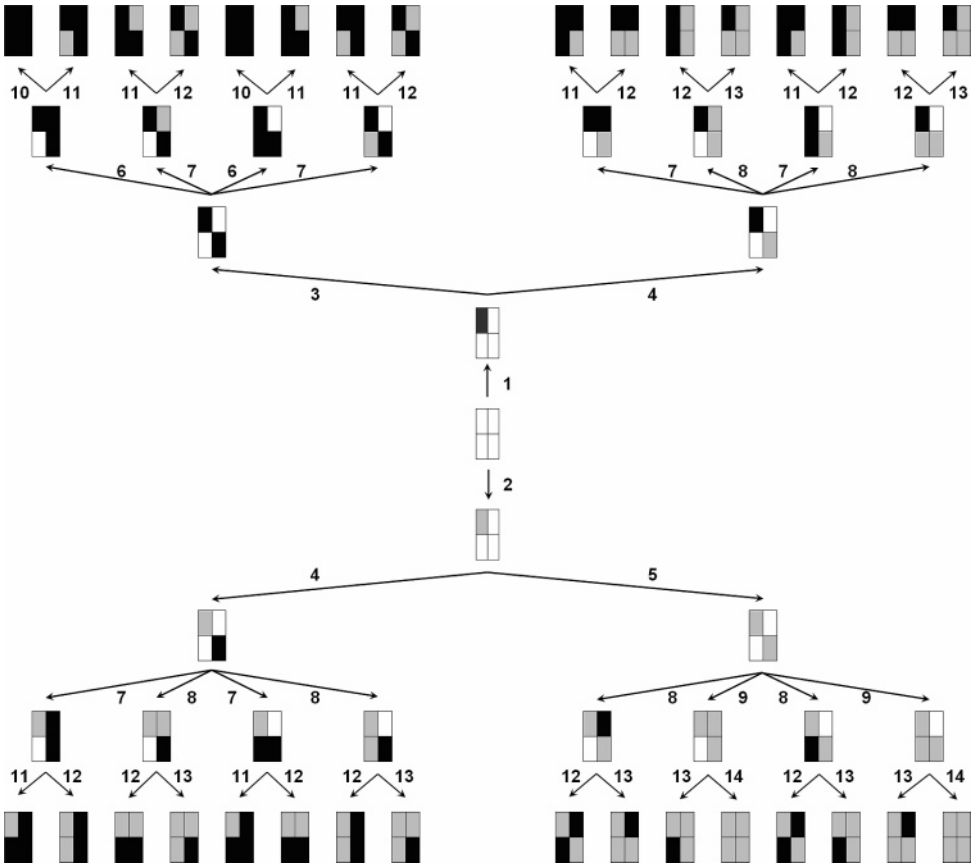

[a] White boxes represent free binding sites, and black boxes and gray boxes represent Δ-**1** and Λ-**1**-loaded binding sites, respectively.

quenching of biotinylated fluorescein upon incorporation in (strept)avidin.[30−32]

In a first attempt to determine the affinity of **1** for (strept)-avidin, spectrophotometric titrations of apoproteins (8.00 μM, 2.400 mL) were carried out at 25 °C in a pH 7.00 buffered aqueous medium (phosphate buffer, $I = 0.15$ M) using circularly polarized light. The ellipticity changes induced by the incremental addition of a *rac*-[Ru(bpy)$_2$(Biot-bpy)]$^{2+}$ (*rac*-**1**) solution in 5.0 μL aliquots (0.25 equiv) were monitored up to 6.0 equiv vs the tetrameric protein in the 250−500 nm range by circular dichroism (CD) spectroscopy. The CD spectra resulting from the titration of *rac*-[Ru(bpy)$_2$-(Biot-bpy)]$^{2+}$ (*rac*-**1**) with avidin are depicted in Figure 2. Very similar results were obtained with streptavidin (data not shown). As the biotinylated guest is racemic, the

(30) Gruber, H. J.; Kada, G.; Marek, M.; Kaiser, K. *Biochim. Biophys. Acta* **1998**, *1381*, 203−212.
(31) Kada, G.; Kaiser, K.; Falk, H.; Gruber, H. J. *Biochim. Biophys. Acta* **1999**, *1427*, 44−48.
(32) Kada, G.; Falk, H.; Gruber, H. J. *Biochim. Biophys. Acta* **1999**, *1427*, 33−43.

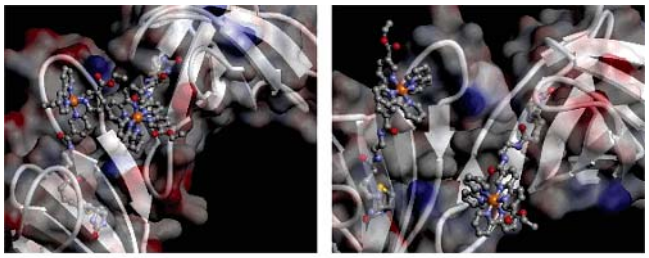

(a) (b)

Figure 1. Results of docking simulations between diastereopure Λ-[Ru(bpy)$_2$(Biot-bpy)]$^{2+}$ (ball-and-stick representation, hydrogen atoms omitted) and a (strept)avidin dimer (transparent solvent accessible surface and schematic secondary structure): (Λ-[Ru(bpy)$_2$(Biot-bpy)]$^{2+}$)$_2$⊂avidin (a); (Λ-[Ru(bpy)$_2$(Biot-bpy)]$^{2+}$)$_2$⊂streptavidin (b).

appearance of a band centered at 313 nm can be attributed to an induced CD signal resulting from second coordination sphere interactions between the host and the guest.

All attempts to analyze the data using the SPECFIT/32 package with up to four independent binding constants (vide supra) failed, as reflected by the lack of convergence of the fitting procedure. We reasoned that the failure to fit the data may be caused by the presence of both diastereomers of the biotinylated coordination complex **1** within a single tetrameric (strept)avidin.

For simplification purposes, let us assume that a second guest enters exclusively the in trans-position to the first guest. In addition, we assume that the remaining two free binding sites in (**1**)$_2$⊂(strept)avidin are identical. If one considers that the affinity of an entering guest **1** depends on the presence or the absence of a guest (as well as its chirality) in an adjacent binding site, there are a total of 14 different binding constants to be fitted for a racemic guest *rac*-**1**. This complex, but simplified, situation is summarized in Scheme 3. In the case of a diastereopure guest, the situation simplifies to afford a total of four binding constants, as summarized in eq 1.

$$\text{(strept)avidin} + x\mathbf{1} \rightleftarrows \mathbf{1}_x\subset\text{(strept)avidin} \qquad (1)$$

$$\beta_x = \frac{[\mathbf{1}_x\subset\text{(strept)avidin}]}{[\text{(strept)avidin}]\cdot[\mathbf{1}]^x} = \prod_{i=1}^{x} K_i \qquad (2)$$

To alleviate the above problem, the spectrophotometric titrations were repeated with the diastereopure biotinylated ruthenium complexes Λ-**1** and Δ-**1**. Typical sets of spectra recorded for the titration of (strept)avidin by complex Λ-**1** and Δ-**1** are depicted in Figure 3. As expected considering the well-documented structural similarity of avidin and streptavidin,[3] they closely resemble each other.

Whereas the free (strept)avidin spectra show weak absorption bands occurring below 300 nm with a positive Cotton effect that are ascribed to tryptophan-centered transitions, both proteins are spectroscopically silent above 310 nm. Upon addition of the Λ-**1** diastereomer, a negative band at 280 nm progressively appears accompanied by a more intense and positive signal centered around 300 nm that tails out in the visible region as broad, albeit much weaker, absorption features with a negative (340−455 nm) and, at higher wavelengths, a positive (455−500 nm) Cotton effect. As the

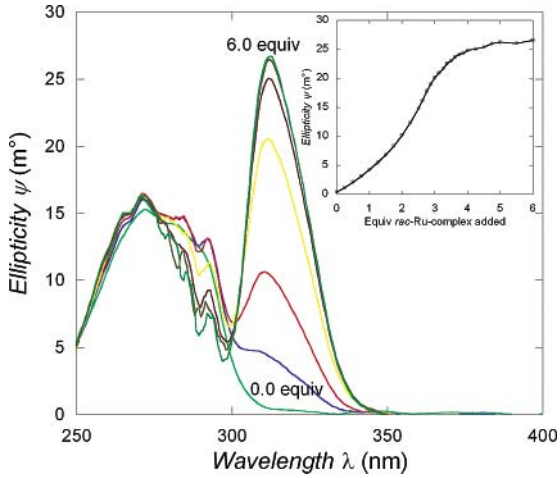

Figure 2. Circular dichroism titration profile obtained for the addition of aliquots of *rac*-**1** to avidin. Inset: Titration profile at 313 nm. (Conditions: I = 0.15 M; KH_2PO_4/Na_2HPO_4; pH = 7.00; T = 298.1 K.)

titration proceeds, the CD-induced absorption bands undergo subtle morphological changes in the UV region, without showing sharply defined isodichroic points. This behavior is best exemplified by the steady intensity increase of the low- at the expense of the high-energy component of the positive envelope peaking at 308 nm (ca. 10 nm shift) at the end of the titration of (strept)avidin. The nonmonotonic variation of the absorbance measured at selected wavelengths (Figure 4) further confirms the one-by-one sequential uptake of the biotinylated ruthenium tris(bipyridine) substrate by the protein.

Despite opposite Cotton effects and some similarities in the general morphology, the spectra pertaining for a given protein (avidin or streptavidin) to both Λ-**1** and Δ-**1** diastereomers are not directly superimposable to the mirror images of each other. The major differences appear in the region around 300 nm. Whereas the positive feature is clearly resolved into two components in the case of the Λ-**1** diastereoisomer (Figure 3a,c), for the Δ-**1** complex, the negative feature evidences no visible splitting (Figure 3b,d). An additional feature that is only observed for the binding of Δ-**1** diastereomer is provided by development of a much weaker band with positive Cotton effect at 331 nm (Figure 3b,d). This electronic transition is characteristic for complex formation since it is absent in the spectrum of free Δ-**1**.

For each system, factor analysis using the singular-value decomposition procedure implemented in the SPECFIT/32 global-analysis software package[33−35] suggests that the entire data sets comprising 27 spectra and 501 evenly distributed wavelengths can be described with no more than five, and possibly only four, eigenvectors without losing information other than instrumental noise. The overall stability constants β_x (eq 2) related to equilibrium (1) were subsequently refined by nonlinear least-squares using Marquardt's algorithm.[36]

(33) Gampp, H.; Maeder, M.; Meyer, C. J.; Zuberbühler, A. D. *Talanta* **1985**, *32*, 95−101.
(34) Gampp, H.; Maeder, M.; Meyer, C. J.; Zuberbühler, A. D. *Talanta* **1985**, *32*, 257−264.
(35) Gampp, H.; Maeder, M.; Meyer, C. J.; Zuberbühler, A. D. *Talanta* **1985**, *32*, 1133−1139.
(36) Marquardt, D. W. *J. Soc. Indust. Appl. Math.* **1963**, *11*, 431−441.

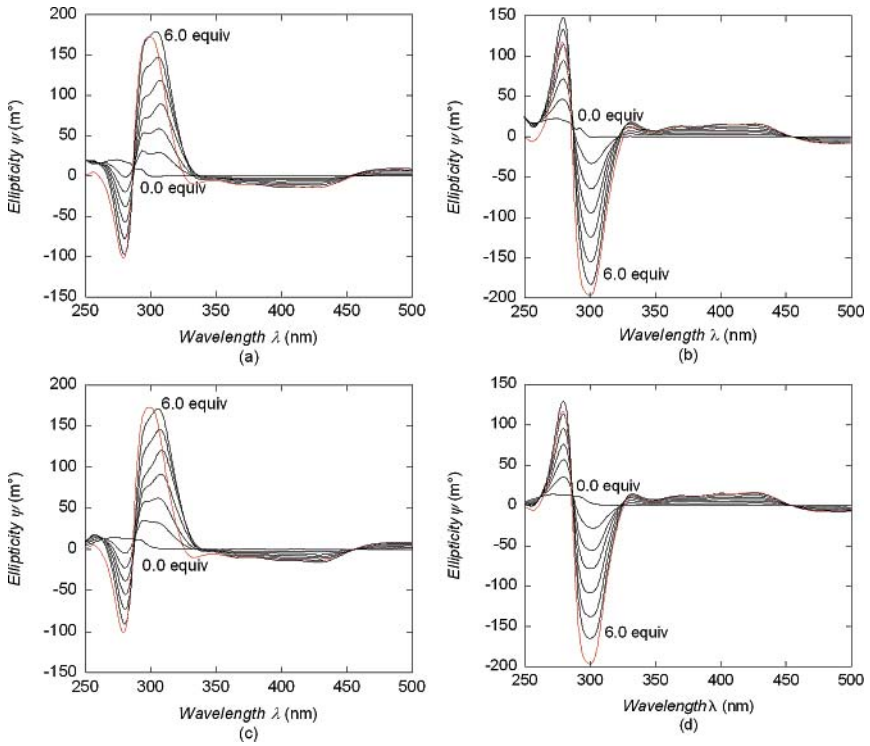

Figure 3. Circular dichroism titration profile obtained for the addition of aliquots of Λ-**1** to streptavidin (a), Δ-**1** to streptavidin (b), Λ-**1** to avidin (c), and Δ-**1** to avidin (d). The red lines correspond to the CD spectra of the diastereopure biotinylated complexes in the absence of (strept)avidin. (Conditions: I = 0.15 M; KH_2PO_4/Na_2HPO_4; pH = 7.00; T = 298.1 K.)

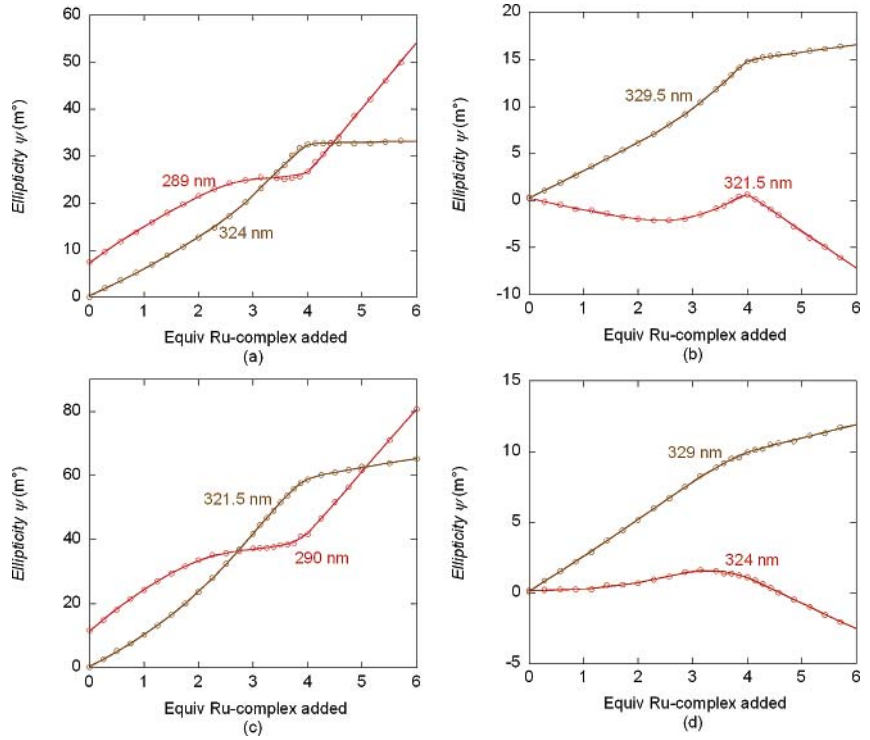

Figure 4. Circular dichroism titration profile at selected wavelengths obtained for the addition of aliquots of Λ-**1** to streptavidin (a), Δ-**1** to streptavidin (b), Λ-**1** to avidin (c), and Δ-**1** to avidin (d). Empty circles: measured data, Full lines: fitted data. (Conditions: I = 0.15 M; KH_2PO_4/Na_2HPO_4; pH = 7.00; T = 298.1 K.)

Considering that both streptavidin and avidin are homotetrameric proteins constructed from identical, single domain subunits consisting of eight-stranded, antiparallel β-barrels, the most obvious chemical model to be considered should include six absorbing species, namely the four inclusion complexes (x = 1−4) in addition to both reactants, **1**, and (strept)avidin, since both display a CD signal in the explored wavelength window. All attempts to analyze the experimental titration data with up to four independent binding constants failed however, as reflected by the lack of convergence of

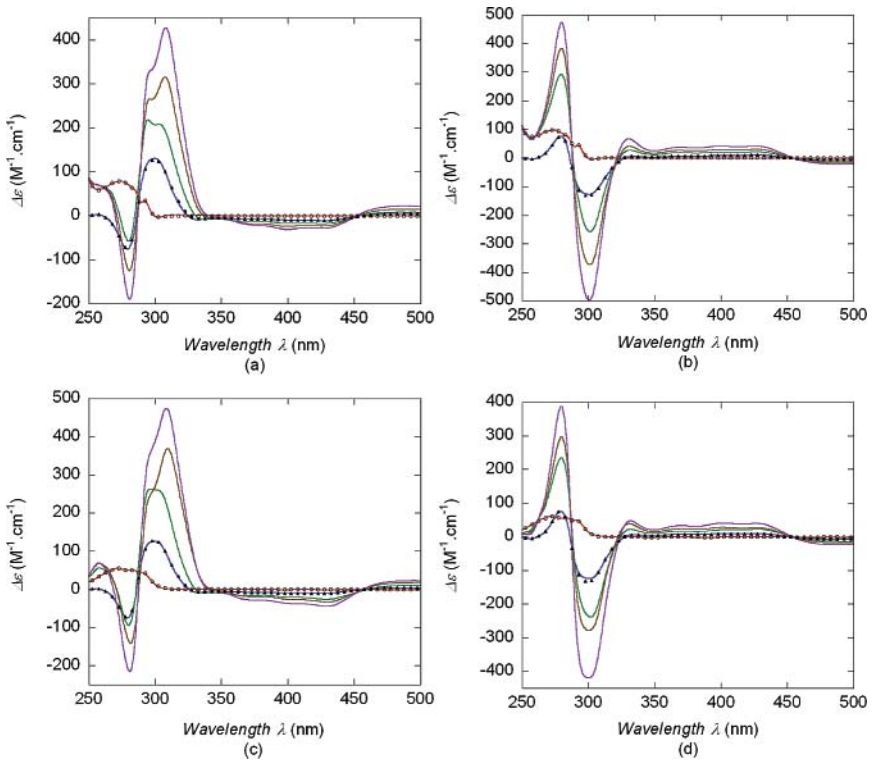

Figure 5. Refined CD spectra for each absorbing species for (Λ-**1**)$_x$⊂streptavidin (a), (Δ-**1**)$_x$⊂streptavidin (b), (Λ-**1**)$_x$⊂avidin (c), and (Δ-**1**)$_x$⊂avidin (d). Key: $x = 0$, red line; $x = 2$, green line; $x = 3$, brown line; $x = 4$, violet line. For comparison, the measured spectra for the host protein and for the biotinylated guest **1** are displayed as open circles and full triangles, respectively, overlaid with the corresponding refined spectra (thin lines).

the fitting procedure. The encountered numerical difficulties are a direct consequence of a very shallow, badly defined error hypersurface and were systematically associated with divergence of the first equilibrium constant β_1.

Hence, various models describing the formation of only three inclusion complexes were evaluated on the basis of the lack-of-fit parameter σ expressed as the residual standard error and by the physical meaning of the calculated CD spectra pertaining to each species. A comparison of the calculated and experimental spectra recorded for the apo-(strept)avidin and complex **1** was of particular value in discarding models with similar σ values that were not statistically different from each other at the 95% probability level according to a Fischer−Snedecor *F*-test.[37] The optimal fit was systematically obtained after excluding β_1 from the set of refined constants and proved also to be significantly superior when compared to a single- and a two-species model. Best estimates of the stepwise binding constants K_x (eq 2) are summarized in Table 1, together with their standard deviations derived from the full variance/covariance matrix.[38] As expected, the refined log β_x values were highly correlated with correlation coefficients systematically exceeding 0.99, while the stepwise constants (log K_x) were only weakly correlated. The highest correlation coefficient in the range of 0.75 was found between log K_1K_2 and log K_3, which is not surprising given the difficulties encountered to estimate log K_1.

Table 1. Summary of Refined Binding Constants between [Ru(bpy)$_2$(Biot-bpy)]$^{2+}$ (**1**) and (Strept)avidin Using a Three Equilibria Model[a] with Standard Deviations in Parentheses

host−guest complex	log K_1K_2	log K_3	log K_4
(Δ-[Ru(bpy)$_2$(Biot-bpy)]$^{2+}$)⊂avidin	15.1(5)	6.8(2)	6.7(1)
(Λ-[Ru(bpy)$_2$(Biot-bpy)]$^{2+}$)⊂avidin	15.7(3)	7.2(1)	7.4(1)
(Δ-[Ru(bpy)$_2$(Biot-bpy)]$^{2+}$)⊂streptavidin	18.9(9)	8.9(2)	8.4(2)
(Λ-[Ru(bpy)$_2$(Biot-bpy)]$^{2+}$)⊂streptavidin	18.8(6)	9.5(2)	8.1(1)

[a] $I = 0.15$ M (KH_2PO_4/Na_2HPO_4), pH = 7.00, and $T = 298.1$ K.

The refined CD spectra corresponding to each absorbing species for the four investigated systems are displayed in Figure 5. Overall, the $\Delta\epsilon$ values calculated for the apoproteins (the host) and free diastereopure complexes are in excellent agreement with the experimentally measured values. Moreover, almost perfect mirror image coincidence was found for the computed spectra of both Λ-**1** and Δ-**1** diastereomers, providing further confidence in the refinement results. A speciation diagram for all four cases studied is presented in Figure 6.

Despite all our attempts (including addition of smaller aliquots of biotinylated complex **1** as well as titration of **1** with aliquots of (strept)avidin), we were unable to determine the first binding constant K_1 for **1**⊂(strept)avidin. Two arguments may be put forward to rationalize this:

One might argue that the impossibility to identify the monobiotinylated complex during the titration is a direct consequence of very similar spectral signatures of both mono-biotinylated **1**⊂(strept)avidin and bis-biotinylated (**1**)$_2$⊂(strept)avidin host−guest complexes that makes them undistinguishable by CD spectroscopy. This argument is plausible considering the high similarity of the four binding

(37) *Commissariat à l'Energie Atomique, Statistique appliquée à l'exploitation des mesures*; Masson: Paris, 1978; Vols. 1−3.
(38) Raymond, K. N.; McCormick, J. M. *J. Coord. Chem.* **1998**, *46*, 51−57.

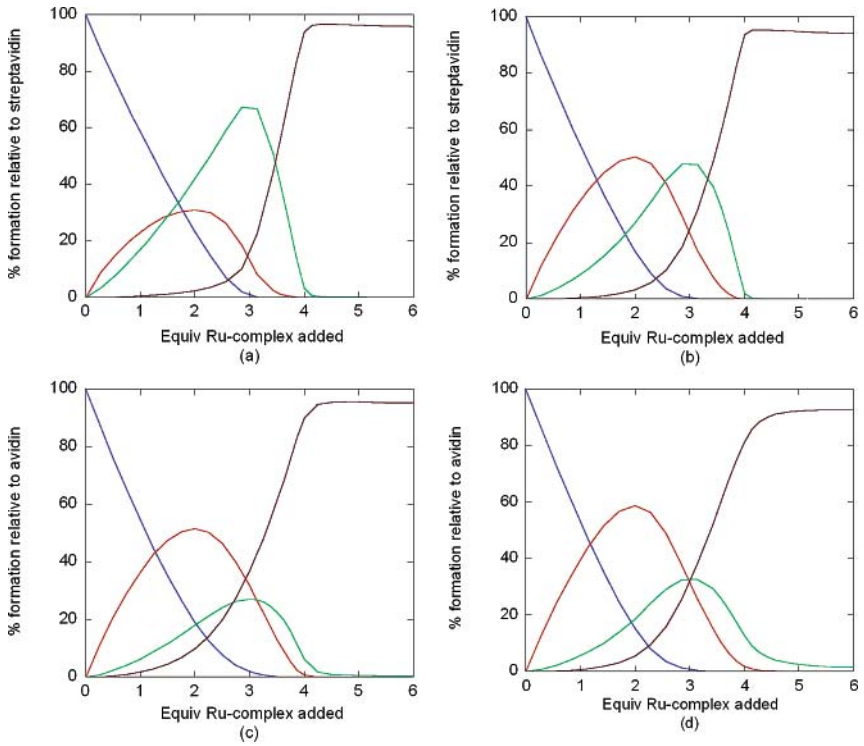

Figure 6. Species distribution diagram for $(\Lambda\text{-}\mathbf{1})_x\subset$streptavidin (a), $(\Delta\text{-}\mathbf{1})_x\subset$streptavidin (b), $(\Lambda\text{-}\mathbf{1})_x\subset$avidin (c), and $(\Delta\text{-}\mathbf{1})_x\subset$avidin (d). Key: $x = 0$, blue line; $x = 2$, red line; $x = 3$, green line; $x = 4$, brown line.

domains found in the crystal structures of both proteins in the loaded and unloaded state. However, analysis of simulated data sets generated by restraining the extinction coefficients of the 1:1 species to be equal or half the $\Delta\epsilon$ values found for the 1:2 complex seems to rule out this hypothesis.

The second sustainable explanation rests on a strongly cooperative[39,40] formation of the $(\mathbf{1})_2\subset$(strept)avidin complex ($K_2 \gg K_1$) so that the free concentration of $\mathbf{1}\subset$(strept)avidin at any stage of the titration remains below the detection limit of the CD spectrophotometer.

A quantitative assessment of cooperativity for the four systems under investigation is complicated by the errors associated with the equilibrium constants and most importantly by the fact that K_1 remains experimentally inaccessible. In the present case, it proved particularly intricate to circumvent this difficulty just by tuning the titration conditions while maintaining the measured signal below the saturation level of the CD detector.[41,42] Although the spectral contribution of the monoadduct $\mathbf{1}\subset$(strept)avidin species to the overall measured CD signal is similar or even below the instrumental noise level, exclusion of β_1 from the chemical model raises some important concerns from a computational standpoint. One of the major issues to be addressed concerns the reliability of the best estimates found for β_2, β_3, and β_4 by the nonlinear least-squares procedure.

To appreciate the extent of the bias on the refined values of the equilibrium constants introduced when the formation constant of a minor species is ignored, a series of artificial data sets with known values of the thermodynamic parameters and molar CD absorption coefficients were generated at different, but constant, noise levels using the simulation routine implemented in Specfit. The details for the simulations are collected in the Supporting Information.

Reagent concentrations and other titration data were chosen so as to reproduce accurately the actual titration conditions. The refined spectra and rounded-off values of the equilibrium constants corresponding to the free components and the $(\mathbf{1})_x\subset$(strept)avidin ($2 \le x \le 4$) species displayed in Figure 3 were used as input for each simulation. As far as the uncharacterized $\mathbf{1}\subset$(strept)avidin species is concerned, the $\Delta\epsilon$ values were arbitrarily set to half the molar CD absorption coefficient calculated for $(\mathbf{1})_2\subset$(strept)avidin, which seems a reasonable assumption considering the similar spectral morphologies displayed by the three inclusion complexes. Subsequent global analyses of the artificial data sets, first with the correct model and then with a submodel ignoring the formation of the minor $\mathbf{1}\subset$(strept)avidin complex, allow one to check the robustness of the minimization algorithm with increasing random noise.

Considering that the standard error in the ellipticity measurements is within <0.1%, as it is the case in all experiments carried out in this work, the maximal concentration of $\mathbf{1}\subset$(strept)avidin does not exceed 4% during the entire titration. The results for this simulation are compiled in Table 2. Excluding β_1 from the model results in a *sizable but approximately constant bias close to 0.25 logarithmic* units

(39) Ercolani, G. *J. Am. Chem. Soc.* **2003**, *125*, 16097−16103.
(40) Perlmutter-Hayman, B. *Acc. Chem. Res.* **1986**, *19*, 90−96.
(41) Dyson, R. M.; Kaderli, S.; Lawrance, G. A.; Maeder, M.; Zuberbühler, A. D. *Anal. Chim. Acta* **1997**, *353*, 381−393.
(42) Dyson, R. M.; Maeder, M.; Neuhold, Y.-M.; Puxty, G. *Anal. Chim. Acta* **2003**, *490*, 99−108.

Table 2. Influence of the Random Noise Level on the Association Constant Values Refined Either for the Complete (Eqs 1−4) or Partial (Eqs 2−4) Models[a]

param	input data for simulation	0.1% noise level
	4 Equilibrium Model	
$\log \beta_1$	8.00	8.2(8)
$\log \beta_2$	19.00	19.1(3)
$\log \beta_3$	28.00	28.2(4)
$\log \beta_4$	36.00	36.2(5)
σ		2.207×10^{-2}
$\Delta\theta_{min/max}$ (mdeg)		$\pm 2 \times 10^{-1}$ [b]
	3 Equilibrium Model	
$\log \beta_2$	19.00	19.2(4)
$\log \beta_3$	28.00	28.3(5)
$\log \beta_4$	36.00	36.3(5)
σ		2.431×10^{-2}
$\Delta\theta_{min/max}$ (mdeg)		$\pm 2 \times 10^{-1}$ [b]

[a] σ: residual standard deviation. $\Delta\theta_{min/max}$: range of the residual ellipticities expressed in millidegrees. [b] The residues are randomly distributed around zero.

which affects the refined β_2, β_3, and β_4 equilibrium constants. Thus, the values reported in Table 1 that pertain to the analysis of the experimental CD spectra with only three equilibria should be considered spoilt by systematic errors at least as large as the standard errors returned by the Marquardt procedure.

On the basis of of these observations, we conclude that the formation of the (**1**)$_2$⊂(strept)avidin occurs with strong cooperativity, precluding the determination of the first binding constant K_1 for **1**⊂(strept)avidin.

From the data presented in Table 1, there appears to be an enhanced overall stability ($\log \beta_4$) when streptavidin is the host compared to avidin. Considering the respective isoelectronic points of avidin (pI = 10.4) and of streptavidin (pI = 6.4) and the cationic charge of the guest, this difference in affinity may be due to Coulomb interactions combined with the well documented depth of the streptavidin binding pocket. In terms of chiral discrimination properties of the host protein, avidin displays a modest preference for Λ-**1**, whereas streptavidin binds nearly indiscriminately both Λ-**1** and Δ-**1**. Considering the large standard deviations, this last conclusion is subject to caution however.

It is interesting to note that, in the area of artificial metalloenzymes for enantioselective catalysis, streptavidin systematically outperforms avidin in terms of enantiodiscrimination.[16−19]

Conclusions. With the aim of probing second coordination sphere interactions upon incorporation in (strept)avidin, diastereopure biotinylated ruthenium tris(bipyridine) complexes (Λ or Δ)-[Ru(bpy)$_2$(Biot-bpy)]$^{2+}$, (Λ or Δ)-**1**, were synthesized. Using circular dichroism spectroscopy, the stepwise stability constants were determined for the supramolecular complexes: (Δ-[Ru(bpy)$_2$(Biot-bpy)]$^{2+}$)$_x$⊂avidin, (Λ-[Ru(bpy)$_2$(Biot-bpy)]$^{2+}$)$_x$⊂avidin, (Δ-[Ru(bpy)$_2$(Biot-bpy)]$^{2+}$)$_x$⊂streptavidin, and (Λ-[Ru(bpy)$_2$(Biot-bpy)]$^{2+}$)$_x$⊂streptavidin (x = 1−4). Critical analysis of the refined thermodynamic data fully supports the conclusion of a strong cooperativity between the first and the second binding events, thus precluding the refinement of the first binding constant. The overall stability constants ($\log \beta_4$ = 28.6, 30.3, 36.2, and 36.4, respectively) point toward a pronounced difference in affinity between avidin and streptavidin for the dicationic guest **1** as well as modest enantiodiscrimination properties with avidin as host. These data demonstrate that the stability of the biotin−(strept)avidin couple decreases dramatically in the presence large biotinylated probes devoid of long spacers between the biotin anchor and the probe. This may be particularly relevant when working at high dilutions, as the biotin−(strept)avidin "molecular velcro" may no longer ensure quantitative incorporation of the large biotinylated probe in (strept)avidin.

Using a rigid (strept)avidin host, docking simulations with (Λ or Δ)-**1** yield a qualitative three-dimensional model, suggesting that the coordination complex is located on the surface of (strept)avidin rather than in the binding pocket. However, the tetrameric nature of the protein provides a large contact area between the host and the guest. Current efforts are focused on crystallization of the host⊂guest complex.

In a broader perspective, this study reveals the versatility of CD spectroscopy to probe complex binding equilibria, allowing the unambiguous identification of individual binding events—perhaps hard to identifiy with other nonchiroptical techniques.

Acknowledgment. We thank Prof. C. R. Cantor for the streptavidin gene and Belovo Egg Science and Technology for a generous gift of egg white avidin. Prof. A. von Zelewsky is thanked for his help during the preparation of diastereopure **1**. This work was funded by the Swiss National Science Foundation (Grants FN 620-57866.99 and FN 200021-105192/1 as well as NRP 47 "Supramolecular Functional Materials"), CERC3 (Grant FN20C321-101071), the Roche Foundation, and the Canton of Neuchâtel, as well as FP6 Marie Curie Research Training Network (IBAAC network, MRTN-CT-2003-505020).

Supporting Information

(Strept)avidin as Host for Biotinylated Coordination Complexes: Stability, Chiral Discrimination and Cooperativity

Andreas Loosli,[‡] Untung Edy Rusbandi,[‡] Julieta Gradinaru,[‡] Klaus Bernauer,[‡] Carl Wilhelm Schlaepfer,[◊] Michel Meyer[§], Sylwester Mazurek,[‡ζ] Marjana Novic[ζ] and Thomas R. Ward[‡]*

[‡]Institute of Chemistry, University of Neuchâtel, Av. Bellevaux 51, CP 2, CH-2007 Neuchâtel, Switzerland; [◊]Institute of Inorganic Chemistry, University of Fribourg, Pérolles, CH-1700 Fribourg, Switzerland; [§]Laboratoire d'Ingénierie Moléculaire pour la Séparation et les Applications des Gaz (LIMSAG, UMR 5633 du CNRS), Université de Bourgogne, Faculté des Sciences, 6 Boulevard Gabriel, F-21100 Dijon, France and [ζ]Laboratory of Chemometrics, National Institute of Chemistry, Hajdrihova 19, SI-1001 Ljubljana, Slovenia

thomas.ward@unine.ch

Experimental Part

Synthesis of Ligand and Complexes

The biotinylated ethylenediamine (**2**) and activated ester (**3**) were synthesized according the Li & co-workers[1] and Somlai & co-workers' procedures[2]. As well as the synthesis of *Δ*-[$Ru(bpy)_2(py)_2$][(+)-O,O'-dibenzoyl-*D*-tartrate] · $12H_2O$, which was achieved by von Zelewsky's method[3]. However, the basic condition (pH = 8–9) is needed to achieve a good solubility of tartaric acid.

Biot-bpy (**4**)

A solution of biotinylated ethylenediamine (**2**) (100 mg, 0.31 mmol) and NEt_3 (130 μL, 0.93 mmol, 3 eq) in DMF (15 mL) was added dropwise to a solution of activated ester (**3**) (272 mg, 0.62 mmol, 2 eq) in DMF (15 mL), which led to a change of yellow to orange-yellowish. Upon stirring the reaction mixture (rt, 3 d), the solvent was evaporated. The residue was purified by washing with ether, cold CH_2Cl_2 and cold CH_3CN. The resulting solid (Biot-bpy (**4**)) was dried *in vacuo* (yield: 118 mg, 0.22 mmol, 70%).

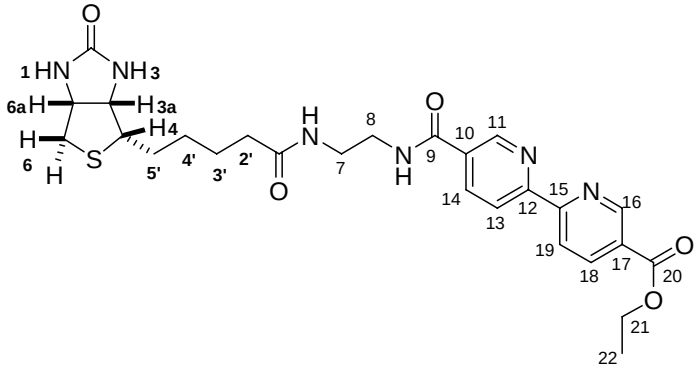

^{1}H NMR (400.00 MHz, DMSO-d_6), δ [ppm]: 1.27-1.63 (m, CH_2, 6H, H-3' & H-4' & H-5'), 1.37 (t, *J* = 7.1 Hz, CH_3, 3H, H-22), 2.09 (t, *J* = 7.3 Hz, CH_2, 2H, H-2'), 2.56 (d, *J* = 12.4 Hz, CH_2, 1H, H-6), 2.79 (dd, *J* = 5.1 Hz & *J* = 12.4 Hz, CH_2, 1H, H-6), 3.26-3.29 (m, CH_2, 4H,

en, H-7, H-8), 3.02-3.07 (m, CH, 1H, H-4), 4.08-4.11 (m, CH, 1H, H-3a), 4.26-4.29 (m, CH, 1H, H-6a), 4.39 (q, *J* = 7.1 Hz, CH_2, 2H, H-21), 6.35 (s, biotin, NH, 1H, H-1), 6.42 (s, biotin, NH, 1H, H-3), 7.95 (t, *J* = 5.5 Hz, amide NH, 1H), 8.36-8.39 (m, bpy, CH, 1H, H-14), 8.45-8.48 (m, bpy, CH, 1H, H-18), 8.53-8.60 (m, bpy CH, 2H, H-19 & H-13), 8.81 (t, *J* = 5.6 Hz, amide NH,1H), 9.13 (s, bpy, CH, 1H, H-11), 9.20 (s, bpy, CH, 1H, H-16)

^{13}C NMR (100.58 MHz, DMSO-d_6), δ [ppm]: 15.0 (CH_3, C-22), 26.1 (CH_2,C-5'), 28.9 & 29.0 (CH_2, C-3' & C-4'), 36.1 (CH_2, C-2'), 38.9 & 40.2 (en, CH_2, C-7 &C-8), 40.7 (C-6), 56.2 (C-4), 60.0 (C-6a), 61.9 (C-3a), 62.2 (CH_2, C-21), 121.7 & 121.8 (bpy, CH, C-19 & C-13),137.3 & 139.1 (bpy, CH, C-18 & C-14), 149.4 & 150.9 (bpy, CH, C-16 & C-11), 127.0 & 131.5 (bpy, C_{ter}, C-17 & C-10), 156.7 & 158.7 (bpy, C_{ter}, C-12 & C-15) 163.6 (biot, C_{ter}, C-2) 165.4 (C_{ter}, C-9 & C-20) 173.3(biot, C_{ter}, C-1').

MS ESI (positive mode), for $C_{26}H_{32}N_6O_5S$, M_w = 540.6 g/mol, m/z: 563.3 (I, 100%, $[M+Na]^+$), ESI (negative mode), m/z: 539.1 (I, 100%, $[M-H]^-$).

rac-$[Ru(bpy)_2(Biot\text{-}bpy)](PF_6)_2$ (*rac*-**1**$(PF_6)_2$)

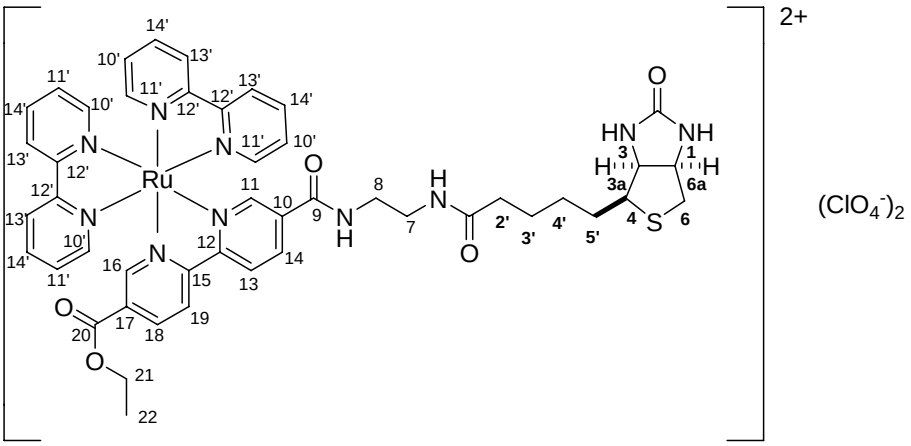

cis-[$Ru(bpy)_2Cl_2$] (89.6 mg, 0.19 mmol) and the biotinylated ligand Biot-bpy (**4**) (100 mg, 0.19 mmol, 1.0 eq) were added to EtOH (30 mL). The solution was heated at reflux temperature (3d) and the solvent was evaporated. The residue was washed three times with ether and redissolved in EtOH (4 mL). To this solution, NH_4PF_6 (127.0 mg, 0.78 mmol, 8.0 eq relative to the formed intermediate product) in H_2O (0.5 mL) was added. The resulting precipitate (*rac*-[$Ru(bpy)_2$(Biot-bpy)]$^{2+}$) was filtered, washed with ether and dried *in vacuo* (yield: 0.18 g, 0.15 mmol, 80%).

^{1}H NMR (400.00 MHz, DMSO-d_6), δ [ppm]: 1.18 (t, *J* = 7.1 Hz, CH_3, 3H, H-22), 1.22-1.63 (m, CH_2, 6H, H-3' & H-4' & H-5'), 2.03 (t, *J* = 7.3 Hz, CH_2, 2H, H-2'), 2.54 (d, *J* = 12.4 Hz, CH_2, 1H, H-6), 2.75-2.80 (m, CH_2, 1H, H-6), 3.02-3.09 (m, CH_2, 1H, H-4), 3.13-3.16 & 3.20-3.22 (m, en, CH_2, 4H, H-7 & H-8), 4.10-4.11 (m, CH, 1H, H-3a), 4.19 (q, *J* = 7.1 Hz, CH_2, 2H, H-21), 4.21-4.23 (m, CH, 1H, H-6a), 6.36 (s, biotin NH, 1H, H-1), 6.40 (s, biotin NH, 1H, H-3), 7.47-7.63 (m, bpy, 4H, H-10'), 7.77-7.87 (m, bpy, 4H, H-14'), 7.91 (d, *J* = 1.6 Hz, biot-bpy 1H), 8.07 (s, biot-bpy, 1H), 8.11 (t, *J* = 5.4 Hz, NH, 1H), 8.15-8.26 (m, bpy, 4H, H-13'), 8.53 (dd, *J* = 1.6 Hz & 8.5 Hz, biot-bpy, 1H), 8.77 (dd, *J* = 1.6 Hz & 8.4 Hz, biot-bpy, 1H), 8.85-8.93 (m, bpy, 4H, H-11'), 9.07 (dd, *J* = 8.5 Hz & 18.3 Hz, biot-bpy, 2H), 9.37 (t, *J* = 5.5 Hz, NH, 1H)

^{13}C NMR (100.58 MHz, DMSO-d_6), δ [ppm]: 13.8 (CH_3, C-22), 25.2 (CH_2, C-5'), 28.0 & 28.1 (CH_2, C-3' & C-4'), 35.1 (CH_2, C-2'), 37.8 & 39.3 (en, CH_2, C-7 &C-8), 39.8 (CH_2, C-6), 55.4 (CH, C-4), 59.2 (CH, C-6a), 61.0 (CH, C-3a), 61.9 (CH_2, C-21), 124.5, 124.6, 125.2, 125.3, 127.9, 128.1, 135.9, 137.6, 138.2, 138.3, 150.7, 151.0, 151.4, 151.6, 151.8, 152.0, 156.1, 156.3, 156.5, 156.7, 157.3 & 159.3 (CH, bpy & biot-bpy), 129.0 & 133.1 (C_{ter}, biot-bpy, C-10 & C-17), 156.1, 156.3, 156.4, 156.7, 157.3, 159.3 (C_{ter}, C-12, C-15, C-12'), 162.2, 162.4, & 162.7 (C_{ter}, CO, C-9, C-20 & C-2), 172.2 (C_{ter}, CO, C-1')

MS (ESI (positive mode), for $C_{46}H_{48}N_{10}O_5RuS$, M_w = 954.0 g/mol), m/z: 1099.1 (I, 18%, $[M+PF_6]^+$), 477.2 (I, 100%, $[M/2]^{2+}$)

MS (ESI (negative mode), for PF_6, M_w = 145.0 g/mol), m/z: 145.1 (I, 100%, $[M]^-$)

UV-Vis (EtOH), λ[nm] (ε[$M^{-1}cm^{-1}$]): 434 (8120), 287 (63000), 253 (23200)

Δ-[Ru(bpy)$_2$(Biot-bpy)](ClO$_4$)$_2$ (*Δ*-**1**(ClO$_4$)$_2$)

Δ-[Ru(bpy)$_2$(py)$_2$][(+)-O,O'-dibenzoyl-*D*-tartrate] · 12H$_2$O (56.3 mg, 0.049 mmol) and ligand Biot-bpy (**4**) (40 mg, 0.074 mmol, 1.5 eq) were added to a 4-mL ethylene glycol (10% H$_2$O) in a 25-mL flask. The solution was heated (120 °C, 3 h), cooled to room temperature and diluted with H$_2$O (16 mL). The resulting mixture was filtered and purified by ion exchange chromatography (*SP Sephadex C-25*) using sodium perchlorate or potassium nitrate. The elution yielded two main bands. The first band (singly charged product *Δ*-[Ru(bpy)$_2$(Biot-bpy)]$^+$ where Biot-bpy (**4**) is the hydrolyzed ligand carrying one negative charge) was eluted with a 0.05 M NaClO$_4$ (or KNO$_3$ 1%) solution while the second band (desired doubly charged product *Δ*-[Ru(bpy)$_2$(Biot-bpy)]$^{2+}$ **(*Δ*-1)**) was eluted with a 0.2 M NaClO$_4$ (or KNO$_3$ 2%) solution.

MS (ESI (positive mode), for $C_{46}H_{48}N_{10}O_5RuS$, M_w = 954 g/mol), m/z: 478.3 (I, 100%, $[(M/2)+H]^{2+}$)

MS (ESI (negative mode), for NO_3 Mw = 62 g/mol, m/z: 62.1 (I, 100%, $[M]^-$)

UV-Vis (H$_2$O), λ[nm] (ε[$M^{-1}cm^{-1}$]): 434 (8200), 287 (63800), 254 (23200)

CD (H$_2$O), λ[nm] (Δε[$M^{-1}cm^{-1}$]): 488 (-5.7), 427 (10.5), 300 (-131.2), 279 (78.2), 256 (-4.0), 230 (20.5)

Λ-[Ru(bpy)$_2$(Biot-bpy)](ClO$_4$)$_2$ *Λ*-**1**(ClO$_4$)$_2$

Λ-[Ru(bpy)$_2$(py)$_2$][(-)-O,O'-dibenzoyl-*L*-tartrate] · 12H$_2$O (56.3 mg, 0.049 mmol) and ligand Biot-bpy (**4**) (40 mg, 0.074 mmol, 1.5 eq) were added to a 4-mL ethylene glycol (10% H$_2$O) in a 25-mL flask. The solution was heated (120 °C, 3 h), cooled to room temperature and diluted with H$_2$O (16 mL). The resulting mixture was filtered and purified by ion exchange chromatography (*SP Sephadex C-25*) using sodium perchlorate. The elution yielded two main bands. The first band (singly charged product *Λ*-[Ru(bpy)$_2$(Biot-bpy)]$^+$ where Biot-bpy (**4**) is the hydrolyzed ligand carrying one negative charge) was eluted with a 0.05 M NaClO$_4$ solution while the second band (desired doubly charged product *Λ*-[Ru(bpy)$_2$(Biot-bpy)]$^{2+}$ *Λ*-**1**) was eluted with a 0.2 M NaClO$_4$ solution.

MS (ESI (positive mode), for $C_{46}H_{48}N_{10}O_5RuS$, M_w = 954 g/mol), m/z: 477.4 (I, 97%, $[M/2]^{2+}$), 485.4 (I, 96%, $[(M+H_2O)/2]^{2+}$, 1016.8 (I, 100%, $[M+NO_3]^+$), 1032.8 (I, 65%, $[M+NO_3+H_2O]^+$)

MS (ESI (negative mode), for NO_3 Mw = 62 g/mol, m/z: 62.1 (I, 100%, $[M]^-$)

UV-Vis (H$_2$O), λ[nm](ε[M^{-1}cm^{-1}]): 434 (8200), 287 (62200), 254 (24400)

CD (H$_2$O), λ[nm](Δε[M^{-1}cm^{-1}]): 487 (5.3), 427 (-10.3), 300 (128.1), 279 (-72.6), 256 (3.4), 230 (-17.3)

Titration Part

The activity of the host protein was determined using Gruber's protocol based on the fluorescence quenching of biotinylated fluorescein upon incorporation in (strept)avidin.[4-6]

General Considerations

All solutions were prepared and measured at room temperature in a phosphate buffer (pH = 7.0, I = 0.15 M). All aliquots were added using micropipettes. The data were analyzed and fitted using the programs SPECFIT/32.

Aliquots of a Λ- or Δ-$[Ru(bpy)_2(Biot\text{-}bpy)]^{2+}$ (**1**) solution (0.96 mM for Λ-**1** and 0.64 mM for Δ-**1**) were added to (strept)avidin (8 μM initial concentration, 2400 μL, 19.2 nmol) in 0.25 eq steps (5 μL per step, up to 6.0 eq) relative to the tetrameric protein. The CD measurements (250-500 nm, band width 2 nm, step resolution 0.5 nm, response time 4 s, 3 accumulations) were recorded at 50 nm/min after thorough vortex mixing (1 min at rt).

General informations

Absorption Spectrophotometry (UV/Vis)

The measurements were performed on a UVIKON 930 spectrophotometer from Kontron/BioTech (manufacturer exists no more). The sample solutions were introduced in 1 cm quartz cells from Hellma, Müllheim (D). The spectrophotometric data were treated with Excel.

Indications in the spectroscopic data collection: λ_{max} [nm] (ε_{max} [$M^{-1}cm^{-1}$], attribution)

Circular Dichroism (CD)

CD spectra were recorded on a J-710 spectropolarimeter from JASCO, Tokyo (J). The sample solutions were introduced in 1 cm quartz cells from Hellma, Müllheim (D). The spectrophotometric data were treated in Excel.

Indications in the spectroscopic data collection: λ_{max} [nm] ($\Delta\varepsilon_{max}$ [$M^{-1}cm^{-1}$])

SPCFIT/32 Simulation Details

To appreciate the extent of bias on the refined values of the equilibrium constants introduced when the formation constant of a minor species is ignored, a series of artificial data sets with known values of the thermodynamic parameters and absorptivities were generated at different but constant noise levels using the simulation routine implemented in SPECFIT/32.

Reagent concentrations and other titration data were chosen so as to reproduce accurately the actual titration conditions. The refined spectra corresponding to the free components and the (**1**)$_x$⊂(strept)avidin ($2 \leq x \leq 4$) species displayed in Figure 5 were used as input data for each simulation. As far as the uncharacterized **1**⊂(strept)avidin species is concerned, the $\Delta\varepsilon$ values were arbitrarily set to be equal to half of the $\Delta\varepsilon$ calculated for (**1**)$_2$⊂(strept)avidin, which seems a reasonable assumption considering the similar spectral morphologies displayed by the three inclusion complexes. Subsequent global analysis of the artificial data sets, first with the correct model and then with a sub-model ignoring the formation of the minor **1**⊂(strept)avidin complex, allow to check the robustness of the minimization algorithm with increasing random noise.

Referring to these calculations, unbiased estimates of the four association constants in full agreement with the true values were computed as long as the noise level remained below

0.001%, although the concentration of Δ-**1**⊂streptavidin does not exceed 1.5% throughout the titration. With increasing noise level (~0.1%), the same refinement difficulties as those experienced for the real data were encountered, leading to exclude β_1 from the model.

However, the most important outcome was obtained when the simulated data were analyzed with the incomplete model. As long as the spectral contribution is significantly greater than the random noise level, a sizeable but approximately constant bias close to 0.25 logarithmic units affects the refined β_2, β_3, and β_4 equilibrium constants, while the visual examination of the residual plot evidences systematic trends. More surprisingly, the deviation of the parameter estimates from their nominal values become larger and larger as the noise level increases and the contribution of the minor species is vanishing in the spectral background. Unpredictable errors that could be larger than one order of magnitude were obtained for the noisiest data sets (0.1% random noise), while the residues were approximately randomly distributed around zero.

It has therefore to be concluded that occurrence of minor species throughout a single titration results not only in poorly defined spectra and equilibrium constants for those species, but more importantly, the entire global nonlinear least-squares analysis fails to produce reliable precise estimates of the unknown parameters corresponding to the major species. The effective rank deficiency evidenced by the singular value decomposition is a direct consequence of the unavoidable experimental noise[7,8]. Thus, the values reported in Table 1 that pertain to the analysis of the experimental CD spectra with only three equilibria, should be considered as approximate and spoilt by systematic errors at least as large as the standard errors returned by the Marquardt procedure [9].

Pertinent results of the singular value decomposition (number of significant eigenvalues) and subsequent nonlinear least-squares refinement of the artificial data sets to which a constant noise level has been superimposed, are summarized in Table S1. As can be seen in

Table S1 and Table 2, if the standard error in the ellipticity measurements is within < 0.1%, as it is the case in all experiments carried out in the present work, it is then safe to trust that the maximal concentration of **1**⊂(strept)avidin does not exceed 4% during the entire titration. Most importantly, this higher limit is a sufficient criterion to assess the cooperative formation of the (**1**)$_2$⊂(strept)avidin adduct starting from the *apo*-protein.

Table S1. Influence of the random noise level on the association constant values refined either for the complete (equilibrium 1 to 4) or partial (equilibrium 2 to 4) models[a]

Noise level	0%	0.001%	0.01%	0.1%	0.2%	0.5%
Nb. of factors	5	5	5	4	4	3
			4 equilibrium model			
log β_1	8.002(3)	8.01(3)	8.2(2)	8.2(8)	< 0[b]	<0[b]
log β_2	19.0000(5)	19.000(5)	19.00(5)	19.1(3)	18.7(4)	20(1)
log β_3	28.0000(7)	28.000(7)	28.00(7)	28.2(4)	27.7(5)	30(1)
log β_4	36.0000(9)	36.000(9)	36.00(8)	36.2(5)	35.7(5)	38(1)
σ	2.337×10^{-5}	2.286×10^{-4}	2.27×10^{-3}	2.207×10^{-2}	2.843×10^{-2}	1.1×10^{-1}
$\Delta\theta_{min/max}$ (m°)	$\pm 2.3 \times 10^{-4}$ [c]	$\pm 2.3 \times 10^{-3}$ [c]	$\pm 2.3 \times 10^{-2}$ [c]	$\pm 2 \times 10^{-1}$ [c]	$\pm 5 \times 10^{-1}$ [c]	± 1 [c]
			3 equilibrium model			
log β_2	19.2(1)	19.2(2)	19.2(2)	19.2(4)	19.2(4)	21(1)
log β_3	28.2(2)	28.2(2)	28.2(2)	28.3(5)	28.2(5)	30(1)
log β_4	36.2(2)	36.2(2)	36.2(2)	36.3(5)	36.3(6)	39(1)
σ	7.240×10^{-3}	7.363×10^{-3}	7.837×10^{-3}	2.431×10^{-2}	2.972×10^{-2}	1.157×10^{-2}
$\Delta\theta_{min/max}$ (m°)	–0.03/0.075 [d]	–0.03/0.075 [d]	–0.03/0.075 [d]	$\pm 2 \times 10^{-1}$ [c]	$\pm 5 \times 10^{-1}$ [c]	± 1 [c]

[a] σ : residual standard deviation; $\Delta\theta_{min/max}$: range of the residual ellipticities expressed in millidegrees. [b] The refinement procedure converges but β_1 is poorly defined and becomes negative (multiple minima). The calculated spectra become unrealistic although the estimates of β_2–β_4 are well defined and unique. [c] The residues are randomly distributed around zero. [d] The plot of residues shows systematic trends.

Simulations for the streptavidin/*Δ*-1 system

Simulated data sets were generated with SPECFIT/32 using a constant noise level and the following conditions:

$[\text{streptavidin}]_0 = 7 \times 10^{-6}$ M

$[\Delta\text{-}\mathbf{1}]_0 = 9.6 \times 10^{-4}$ M

Initial volume of streptavidin solution: $V_0 = 2400$ μL.

The solution of ruthenium complex *Δ*-**1** is added in 0.005 mL increments up to 26 aliquots.

Equilibrium constants derived from Table 1 were rounded off. Values were as follows:

streptavidin + *Δ*-**1** ⇆ (*Δ*-**1**)⊂streptavidin	$\log \beta_1 = 8$	(1)
streptavidin + 2 *Δ*-**1** ⇆ (*Δ*-**1**)$_2$⊂streptavidin	$\log \beta_2 = 19$	(2)
streptavidin + 3 *Δ*-**1** ⇆ (*Δ*-**1**)$_3$⊂streptavidin	$\log \beta_4 = 28$	(3)
streptavidin + 4 *Δ*-**1** ⇆ (*Δ*-**1**)$_4$⊂streptavidin	$\log \beta_4 = 36$	(4)

Figure S1 shows a distribution diagram of the various species formed under these conditions during the simulated experiment.

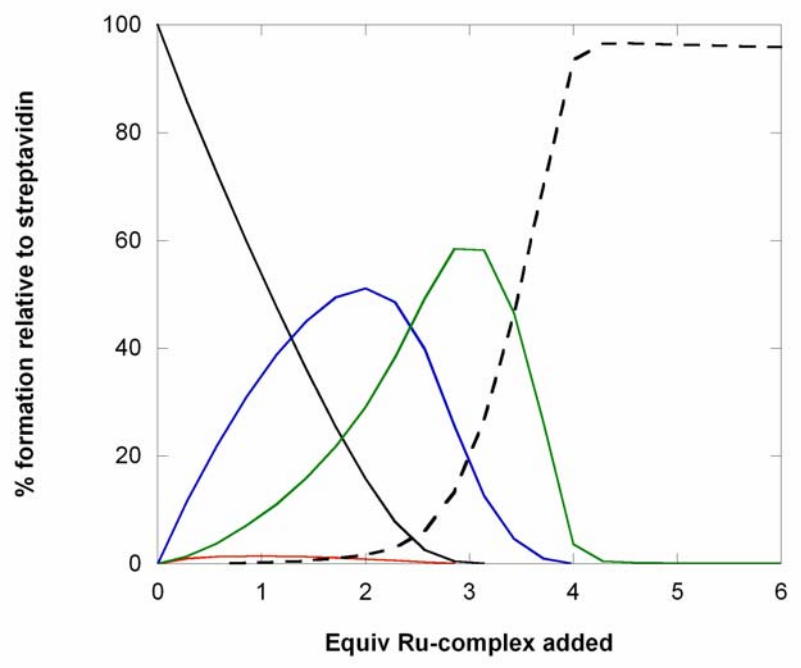

Figure S1. Species distribution diagram calculated for the above mentioned conditions (For each absorbing species for (Δ-[Ru(bpy)$_2$(Biot-bpy)]$^{2+}$)$_x$⊂streptavidin ((Δ-**1**)$_x$⊂streptavidin). *x* = 0: black solid line, *x* = 1:red line, *x* = 2: blue line, *x* = 3: green line and *x* = 4: black dotted line.The fraction of the (Δ-**1**)⊂streptavidin species does not exceed 1.4%.

The individual CD spectra corresponding to each species used to construct the artificial data are displayed in Figure S2. The Δε for (Δ-**1**)⊂streptavidin were deduced from the experimentally refined spectra obtained for (Δ-**1**)$_2$⊂streptavidin by dividing the corresponding $\Delta\varepsilon$ values by a factor of 2.

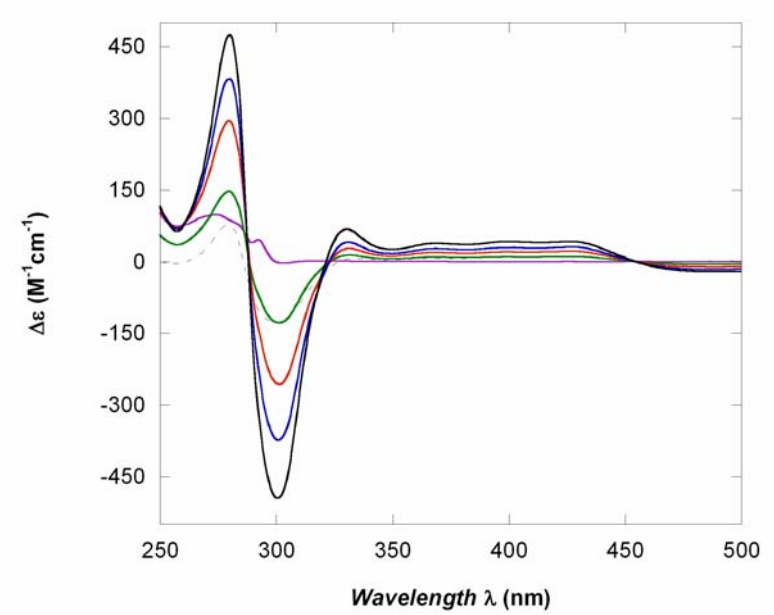

Figure S2. Fixed CD spectra used to generate the artificial data sets. For each absorbing species for (Δ-[Ru(bpy)$_2$(Biot-bpy)]$^{2+}$)$_x$⊂streptavidin ((Δ-**1**)$_x$⊂streptavidin). x = 0: violet line, x = 1: green line, x = 2: red line, x = 3: blue line and x = 4: black solid line. The spectrum of Δ-**1** is displayed as a dotted black line.

(1) Li, Z.; Ortega-Vilain, A.-C.; Patil, G. S.; Chu, D.-L.; Foreman, J. E.; Eveleth, D. D.; Powers, J. C. *J. Med. Chem.* **1996**, *39*, 4089-4098.
(2) Somlai, C.; Berenyi, M.; Maroy, P. *Z. Naturforsch* **1993**, *48(4)*, 511-516.
(3) Hua, X.; von Zelewsky, A. *Inorg. Chem.* **1995**, *34*, 5791-5797.
(4) Kada, G.; Kaiser, K.; Falk, H.; Gruber, H. J. *Biochim. Biophys. Acta* **1999**, *1427*, 44-48.
(5) Kada, G.; Falk, H.; Gruber, H. J. *Biochim. Biophys. Acta* **1999**, *1427*, 33-43.
(6) Gruber, H. J.; Kada, G.; Marek, M.; Kaiser, K. *Biochim. Biophys. Acta* **1998**, *1381*, 203-212.
(7) Dyson, R.M.; Maeder, M.; Neuhold, Y.-M.; Puxty, G. *Anal. Chim. Acta* **2003**, *490*, 99-108.
(8) Dyson, R. M.; Kaderli, S.; Lawrance, G. A.; Maeder, M. *Anal. Chim. Acta* **1997**, *353*, 381-393.
(9) Marquardt, D. W. *J. Soc. Ind. Appl. Math.* **1963**, *11*, 431-441.